

Light piping driven photosynthesis in the soil: low-light adapted active photosynthetic apparatus in the under-soil hypocotyl segments of bean (*Phaseolus vulgaris*)

Andrea Kakuszi¹, Éva Sárvári², Ádám Solti², Gyula Czégény³, Éva Hideg³, Éva Hunyadi-Gulyás⁴, Károly Bóka¹ and Béla Böddi^{1*}

¹ Department of Plant Anatomy, Institute of Biology, Eötvös Loránd University, Pázmány P. s. 1/c, Budapest, H-1117 Hungary

² Department of Plant Physiology and Molecular Plant Biology, Institute of Biology, Eötvös Loránd University, Pázmány P. s. 1/c, Budapest, H-1117 Hungary

³ Department of Plant Biology, Institute of Biology, University of Pécs, Ifjúság u. 6., Pécs, H-7624 Hungary

⁴ Institute of Biochemistry, Biological Research Centre of the Hungarian Academy of Sciences, Temesvári krt. 62., Szeged, H -6726 Hungary

*Corresponding author, email: belaboddi@ttk.elte.hu, phone number: +36-1-2090555/8656

Abbreviations:

sampling regions: L – leaf, AS – above-soil hypocotyl, US-1 – under-soil hypocotyl segment at 0-2 cm depth, US-2 – under-soil hypocotyl segment at 2-4 cm depth; Chl – chlorophyll; Pchl_{id} – protochlorophyllide; PS – photosystem; LHC – light harvesting complex; PFD – photon flux density; ROS – reactive oxygen species; PIP – plasma membrane intrinsic protein; Y(II) – photochemical quantum yield of PSII; Y(NPQ) – regulated non-photochemical quantum yield; Y(NO) – non-regulated non-photochemical quantum yield; Φ_{NF} – participation of non-functional PSII reaction centers in the excitation energy

Abstract

Photosynthetic activity was identified in the under-soil hypocotyl part of 14-day-old soil-grown bean plants (*Phaseolus vulgaris* L. cv. Magnum) cultivated in pots under natural light-dark cycles. Electron microscopic, proteomic and fluorescence kinetic and imaging methods were used to study the photosynthetic apparatus and its activity. Under-soil shoots at 0-2 cm soil depth featured chloroplasts with low grana and starch grains and with pigment-protein compositions similar to those of the above-soil green shoot parts. However, the relative amounts of photosystem II (PSII) supercomplexes were higher; in addition a PIP-type aquaporin protein was identified in the under-soil thylakoids. Chlorophyll-*a* fluorescence induction measurements showed that the above- and under-soil hypocotyl segments had similar photochemical yields at low ($10\text{-}55 \mu\text{mol photons m}^{-2} \text{s}^{-1}$) light intensities. However, at higher photon flux densities the electron transport rate decreased in the under-soil shoot parts due to inactivation of the PSII reaction centers. These properties show the development of a low-light adapted photosynthetic apparatus driven by light piping of the above-soil shoot. The results of this paper demonstrate that the classic model assigning source and sink functions to above- and under-soil tissues is to be refined, and a low-light adapted photosynthetic apparatus in under-soil bean hypocotyls is capable of contributing to its own carbon supply.

Keywords

light piping, greening, chlorophyll-protein complex, chlorophyll fluorescence, aquaporin

1. Introduction

Most plants have under-soil shoot region which is exposed either to low light filtered by the soil or is fully shaded. Thus the latter tissues develop in full darkness [1] and show etiolation symptoms [2]. Their chlorophyll (Chl) biosynthesis is arrested at the conversion of protochlorophyllide (Pchl_{ide}) to chlorophyllide catalyzed by the light-dependent NADPH:protochlorophyllide oxidoreductase enzyme (LPOR; EC 1.3.1.33) [3]. Etioplasts develop, the inner membranes of which contain Pchl_{ide} forms [4]. The Pchl_{ide} forms have usually been studied in leaves [5] or stem-related organs [6] of dark-grown laboratory plants which are good models to study the Chl biosynthesis. Pchl_{ide}₆₃₃ and Pchl_{ide}₆₅₄₋₆₅₅ forms were detected in the under-soil shoot (epicotyl) segments of pea grown in pots under natural light-dark cycles [2]; the spectral properties of these forms were similar to those of etiolated plants. Close to the soil surface (at 0-3 cm depth), however, the pea epicotyls had Chl pigments in parallel with the decreasing amounts of Pchl_{ide} [2]. The under-soil segments of bean hypocotyls contained Pchl_{ide} and Chl pigments, too [7]. However, Chls were detected in hypocotyls even in 5 cm soil depths. This difference has been explained by light piping of the hypocotyl in which a central cavity develops [7]; however, the intensity of the piped light is very low - it is about 10% of the incident light.

Photosynthetic acclimation of plants grown under low light intensities is a well-known phenomenon [10,11]. Characteristic changes in the Chl-protein composition of the leaves take place: the relative amount of the photosystem II (PSII) and its light-harvesting antenna (LHCII) increases [10,11] and as a consequence, the Chl-*a* to Chl-*b* ratio decreases. In the chloroplasts the grana stacks are higher and broader than those of the high-light adapted plants [12,13]. Besides of leaf photosynthesis, the contribution of the photosynthetic activity of stems – including even woody stems – is important [14,15]. The presence of chloroplasts was described in the cortex and in the pith regions of twigs [16]. Radial light transmittance was reported with decreasing photon flux density (PFD) gradient from the twig surface towards its central pith allowing photosynthetic activity; the quantum efficiency of PSII was found decreasing towards the central pith [17]. Although lengthwise light piping seems to be obvious in stems, we could not find direct measurements about this phenomenon; only microscopic observations were published [18]. The lengthwise light piping is effective in stems having hollow pith; this was described in our previous work in which chloroplast containing tissues were observed in under-soil regions of bean hypocotyl [7].

This paper supplies details of the structure and photosynthetic activity of the under-soil bean hypocotyl. The aim of this work was to investigate whether the under-soil chlorenchyma-like tissues have photosynthetic activity. The presence of stomata was detected with scanning electron microscopy, chloroplasts ultrastructure was studied with transmission electron microscopy, the chlorophyll-protein complexes were analyzed with proteomics and the photosynthetic electron transport was studied with variable chlorophyll fluorescence.

2. Materials and methods

2.1. Plant material

Seeds of bush bean (*Phaseolus vulgaris* L. cv. Magnum, Rédei Kertimag Ltd., Réde, Hungary) were soaked in running tap water for 2 hours then pre-germinated in Petri dishes in darkroom at 23°C. After 3 days, the seedlings had 1 cm radicle and were planted under dim green light into pots (planting depth: 4 cm) in potting soil (ASB-Greenworld, pH 5.0-6.5, Zár, Czech Republic). The plants were grown under natural light-dark cycles for 14 days in the laboratory window where the maximal daily PFD varied between 100 and 600 $\mu\text{mol photons m}^{-2} \text{ s}^{-1}$. The plants were watered every second day from the bottom thus the soil structure around the shoots was undisturbed. 14 days after sowing, the plants had a 12-15 cm above-soil shoot (including a 4-5-cm-long hypocotyl part) and an under-soil hypocotyl of 7-8 cm (during the development of the root system, the root neck moved deeper into the soil). The hypocotyls were labeled at the soil surface level before the pots were transferred into darkroom where the plants were taken out from the soil under dim green light. Their under-soil hypocotyl parts were rinsed to remove soil particles. Samples were taken from the leaves (L) and from the following shoot sections: the hypocotyl section right above the soil surface (AS); the under-soil hypocotyl region at 0-2 cm depth (US-1) and between 2 and 4 cm depths (US-2). The samples were collected under the above mentioned dim green light.

2.2. Electron microscopy

For transmission electron microscopy, thin slices (1-1.5 mm) of the halved hypocotyls were immediately immersed into fixative, 2% glutaraldehyde in 0.01 M phosphate buffer pH 7.2, and cut radially into small pieces and fixed for 2 hours. After careful rinsing with the buffer, samples were postfixed for 3 hours in 1% OsO₄ dissolved in the buffer. Tissue pieces rinsed with buffer, dehydrated with increasing ethanol series, were infiltrated and embedded in Durcupan resin. Ultrathin sections (70 nm) were prepared with a Reichert Jung Ultracut E ultramicrotome and stained with uranyl acetate for 6 minutes and lead citrate for 4 minutes

[19]. Sections were observed with a Hitachi 7100 transmission electron microscope (TEM) at 75 kV accelerating voltage.

To take scanning electron micrographs, native samples were imaged (natural scanning electron microscopy) using a Hitachi S-2360N scanning electron microscope (SEM). Samples were observed with 15 kV accelerating voltage and backscattered electron detection.

2.3. Pigment content determination

Samples were homogenized in mortar with 80% (v/v) acetone, centrifuged for 6 minutes at 10000 x g then the pigment contents were determined using an UV-2101PC (Shimadzu, Japan) UV-VIS scanning spectrophotometer. The concentrations were calculated according to Porra et al. [20].

2.4. Proteomics

Plastids and thylakoids were isolated at 0°C on ice. Bean leaves and hypocotyl pieces were homogenized in isolation buffer containing 50 mM 4-(2-hydroxyethyl)-1-piperazineethanesulfonic acid (HEPES)-KOH (pH 7.5), 330 mM sorbitol, 2 mM ethylenediaminetetraacetic acid (EDTA), 2 mM MgCl₂, 0.1% (w/v) bovine serum albumin (BSA) and 0.1% (w/v) Na-ascorbate by Waring Blendor for 3x5 s. The homogenate was filtered on 4 layers gauze and 2 layers Miracloth (Calbiochem-Novabiochem) and centrifuged at 1000 x g (L, AS sections) or 3000 x g (US-1, US-2 sections) for 7 min. The plastid pellet was washed once in the isolation buffer but without BSA and Na-ascorbate. To isolate washed thylakoids, the plastids were osmotically shocked in 10 mM Na₄P₂O₇ (pH 7.5), and centrifuged at 5000 x g for 7 min. Most CF₁ was removed by washing in 5 mM Tricine-(CH₃)₄NOH (pH 7.5), 0.1 M sorbitol (10000 x g, 10 min). Thylakoids were stored in 2 mM Tris-maleate (pH 7.0), 40% glycerol in liquid nitrogen.

The thylakoids were solubilized and the pigment-protein complexes were separated, identified and quantified as described in Sárvári et al. [21] with modification as follows. After solubilisation of thylakoids (0.25 mg Chl ml⁻¹) with 1% (w/v) n-dodecyl-β-D-maltoside on ice for 30 min, first dimension (1.D) electrophoresis (blue-native polyacrylamide gel electrophoresis – BN-PAGE) was run using 5-12% (w/v) acrylamide gradient gels (Mini-Protean, BioRad) with 10-20 μl solubilized thylakoids applied per lane. Electrophoresis was carried out with constant voltage of 40 V (15 min), then 150 V and a maximum of 5 mA per gel at 6°C for approximately 6 h. To analyze the composition of the different complexes, thin slices of native gels were transferred to the top of the second dimension (2.D) denaturing gels according to Laemmli [22] but using 10–18% linear gradient gels modified by adding 10%

glycerol both to the stacking (5%) and separating gels. Staining was done with colloidal Coomassie Blue G-250 [23]. Gels were scanned using an Epson Perfection V750 PRO (Epson, Suwa, Japan) gel scanner. The complexes were identified on the basis of their main protein components using literature data [24,25,26,27]. The quantity of Chl-protein complexes were assessed on the basis of pixel density of the different bands in the 1.D BN-PAGE lanes using Phoretix 4.01 software (Phoretix International, Newcastle upon Tyne, UK). In the case of the complex of photosystem I (PSI) and PSII dimer band, the contribution of PSII dimers was estimated on the basis of the 2.D gel pattern by comparing the density ratio of CP47 apoproteins (PsbB) in the complex band with that in the monomer PSII band. The chlorophyll-protein compositions of thylakoids were compared in the different samples after the total pixel densities of each lane was normalized to identical Chl content.

The total protein composition of the tissues and thylakoids was determined by sodium-dodecyl-sulphate polyacrylamide gel electrophoresis (SDS-PAGE) according to Szentzenstein et al. [28]. Protein content was quantified after SDS-PAGE by comparing the total stain in the lanes to that of a given amount of standard proteins. For western blotting, membrane proteins separated by SDS-PAGE were transferred to Hybound™-C Extra (Amesham-Pharmacia, USA) nitrocellulose membranes in a 25 mM Tris, pH 8.3, 192 mM glycine, 20% (v/v) methanol and 0.02% (m/v) SDS at 4°C using 90 V constant voltage (<0.4 A) for 3 h. The membranes were decorated with rabbit polyclonal antibodies against apoLHCII and D1 (PsbA) protein of PSII (a gift from Dr. Udo Johanningmeier, Bohum Universität, Germany). Antibodies were dissolved in 20 mM Tris-HCl (pH 7.5), 0.15 M NaCl, 1% gelatine. Horseradish peroxidase- (HRP-) conjugated goat-anti-rabbit IgG (BioRad, Inc.) was used to detect bands following the manufacturer's instructions.

2.5. Protein identification by mass spectrometry

A certain spot was cut out of the 2.D SDS-gel of the US-1 segment. After reduction with dithiothreitol and alkylation with iodoacetamide, the sample was digested with trypsin (4 h, 37°C). After extraction of the peptides, the solution was dehydrated and 15 µl 1% formic acid was added. The sample was analyzed with liquid chromatography-tandem mass spectrometry (nanoAcquity UPLC (Waters) coupled to an LCQ-Fleet iontrap mass spectrometer (Thermo)). Raw data were processed by the ProteomDiscoverer (Thermo Fisher Scientific, USA) software. Protein Prospector database was used to identify the peptides with the following parameters: database - UniProtKB.2015.04.16 for Phaseolus; enzyme - trypsin; fixed modifications - carbamidomethyl (C); variable modifications - acetyl (protein N-term), Gln-

>pyro-Glu (N-term Q), oxidation (M); peptide mass tolerance - ± 0.6 kD; fragment mass tolerance - ± 1 kD; maximum missed cleavages - 1.

2.6. Photosynthetic activity measurements

Photosynthetic electron transport and non-photochemical energy dissipation were assessed by measuring Chl fluorescence using pulse-amplitude modulated fluorometry. Variable Chl fluorescence parameters were measured either as average yields (PAM 101-102-103, Heinz Waltz, Effeltrich, Germany) or as fluorescence images (Imaging-PAM with MAXI-head, Heinz Waltz, Effeltrich, Germany). For imaging PAM experiments, plants were kept in darkness for 10 min before removed from the soil and were washed under dim green light. The upper shoot part with leaves was cut and the remaining shoot was placed under the detector. The minimum and maximum fluorescence yields F_0 and F_m were measured in dark adapted samples, before and after a saturating light pulse, respectively. Following this, samples were exposed to $10 \mu\text{mol photons m}^{-2} \text{s}^{-1}$ PFD blue actinic light for 3 min and light acclimated minimum and maximum fluorescence yields F' and F'_m were obtained using a saturating pulse. This was repeated using $55 \mu\text{mol photons m}^{-2} \text{s}^{-1}$ PFD blue actinic light and the quantum yields of PSII photochemistry, $Y(\text{II}) = (F'_m - F)/F'_m$; non-regulated dissimilative processes, $Y(\text{NO}) = F/F_m$; and regulated energy dissipation, $Y(\text{NPQ}) = F/F'_m - Y(\text{NO})$ were calculated for both illuminations conditions according to Klughammer and Schreiber [29]. Different plant parts, such as above and under-soil sections were characterized by averaging yield data of these areas of interest using the Imaging PAM software (ImagingWin v2.46i, Heinz Waltz, Effeltrich, Germany). The above measurements were repeated using three different plants.

In order to characterize inactive PSII reaction centers, a new set of plants were measured using a pulse-amplitude modulated Chl-*a* fluorometer (PAM 101-102-103, Heinz Waltz, Effeltrich, Germany). The difference between the two experiments was the use of stronger, $80 \mu\text{mol photons m}^{-2} \text{s}^{-1}$ PFD white actinic light. The minimal fluorescence (F_0) values were determined by turning on the measuring light (PFD $< 1 \mu\text{mol m}^{-2} \text{s}^{-1}$, modulation frequency: 1.6 kHz). The maximal fluorescence (F_m) values were measured after a 0.7 s flash illumination ($3500 \mu\text{mol m}^{-2} \text{s}^{-1}$ PFD; source: KL 1500 electronic, Schott, Mainz, Germany). The maximal efficiency of the PSII was calculated by the following equation: $F_v/F_m = (F_m - F_0)/F_m$. Non-photochemical quenching related to inactive PSII reaction centers were calculated according to Hendrickson et al. [30] with modifications applied by Solti et al. [31]: $\Phi_{\text{NF}} = 1 - [(F_v/F_m)/(F_{vM}/F_{mM})]$.

2.7. Statistical analysis

Measurements were conducted on $n=5$ biological repetitions. To compare differences between above-soil and under-soil samples, unpaired Student's *t*-tests were performed. To compare multiple parts of the plants, one-way ANOVA tests with Tukey-Kramer multiple comparison *post hoc* tests were performed by InStat v. 3.00 (GraphPad Software, Inc.). The term, 'significantly different', means that the probability for similarity of samples is $P<0.05$.

3. Results

The epidermis of the under-soil shoot was supposed to be special due to the soil environment and the special gaseous exchange in the soil. Scanning electron microscopic images of the AS section showed elongated epidermal cells and paracytic stoma complexes (Fig. 1a). The epidermal cells were shorter and had trapezoid shape in the under-soil region and a few stomata were found also in this US-1 section. The shape of subsidiary cells and guard cells slightly differed; stomata seemed to be more elongated axially (Fig. 1b).

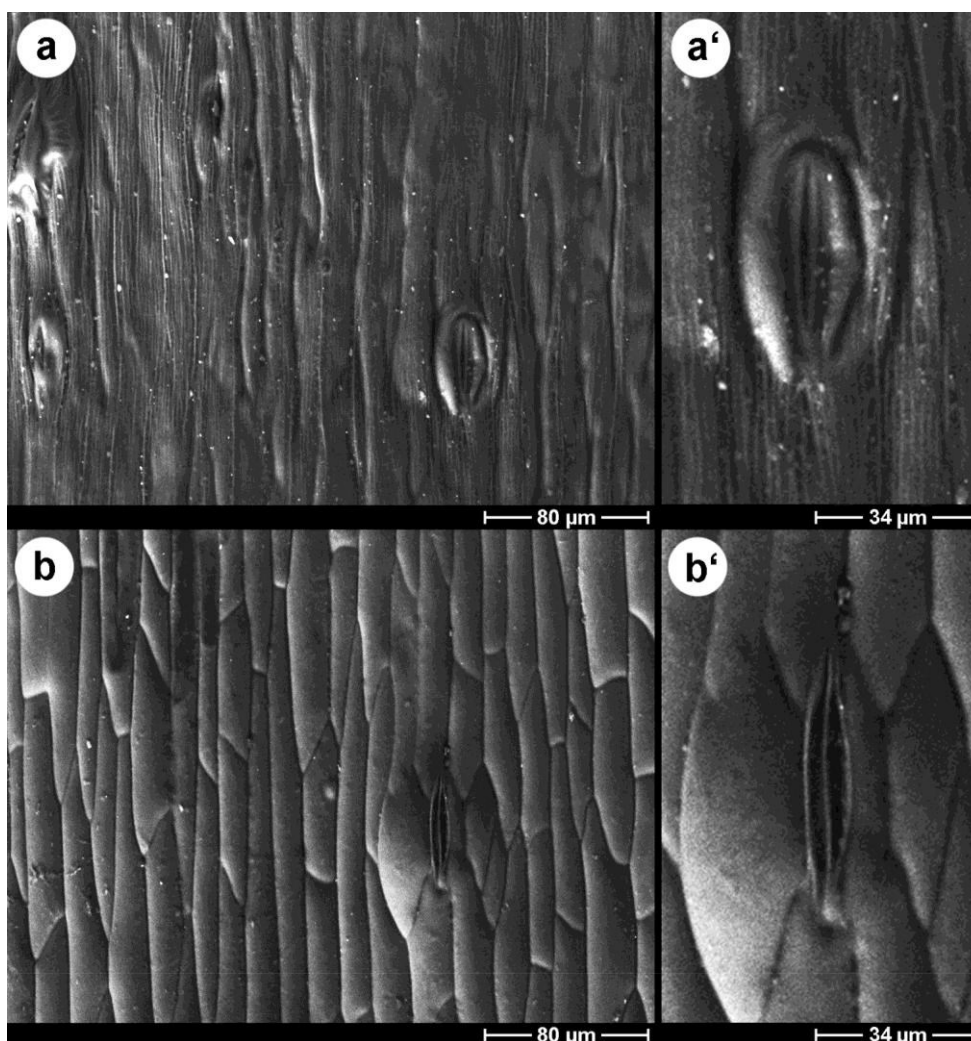


Fig. 1 Scanning electron microscopic images of the epidermis of different hypocotyl sections. The images were taken from 14-day-old bean plants grown in pot under natural light conditions. *a*: hypocotyl section 1 cm above

the soil surface (AS); *a'*: Enlarged detail of (*a*) with a stoma complex; *b*: epidermis of the hypocotyl section 2 cm under the soil surface (US-1); *b'*: enlarged detail of (*b*) with a stoma complex

Leaves and AS hypocotyls contained chloroplasts, the structure of which was characteristic for green plants (not shown). However, in the US-1 segments chloroplasts containing low amount of thylakoids were found. The parenchyma cells of the vascular tissue of the hypocotyls contained small chloroplasts that usually had low grana and starch grains (Fig. 2a); however, plastids with highly stacked thylakoids were also observed (Fig. 2b).

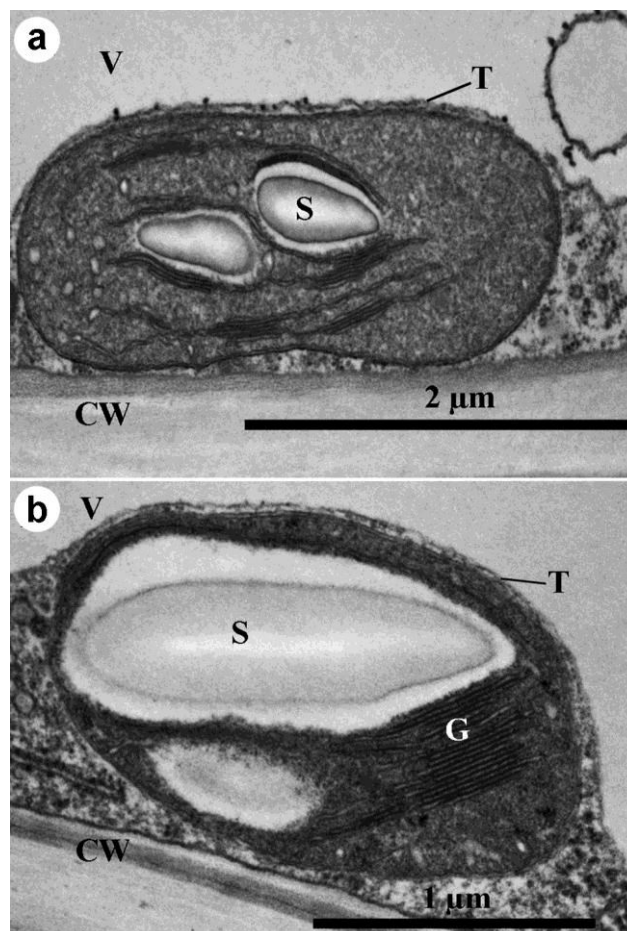


Fig. 2 Transmission electron microscopic images of plastids located in the xylem parenchyma in the uppermost under-soil hypocotyl section (US-1) of 14-day-old bean plant. *a*: plastid with low grana; *b*: chloroplast having high grana and large starch grain. CW – cell wall; V – vacuole; T – tonoplast; S – starch; G – grana

In agreement with the decreased thylakoid contents of the chloroplasts in the under-soil hypocotyl parts, the Chl content was also strongly reduced compared to that of leaves and AS hypocotyl parts (Table 1). A small amount of Chl was detected even in the US-2 region but it reached only 10% of that of the US-1 and only 0.1% of the leaves. The Chl *a/b* ratio of the AS decreased compared to that of leaves, and it decreased further in the under-soil parts reaching

around 1.2 in the US-2 region. Traces of Pchl_{ide} or Pchl were detected only in this latter region, the amounts of which showed high variability. Since the main results of this paper concentrate on the US-1 section and above shoot regions, the presence of Pchl_{ide} or Pchl is not discussed in this paper.

Table 1 Chlorophyll (Chl) contents and Chl-*a* to Chl-*b* ratios of 14-day-old bean leaves (L) and hypocotyl regions. AS - above-soil hypocotyl part; US-1 - under-soil hypocotyl section at 0-2 cm depth; US-2 - under-soil hypocotyl region at 2-4 cm depth. Means and standard deviation values of 5 parallels are shown. To compare the different samples, one-way ANOVAs with Tukey-Kramer *post hoc* tests were performed ($P < 0.05$)

Sample	Chl(<i>a+b</i>) ($\mu\text{mol g}^{-1}$ fresh mass)	Chl <i>a/b</i>
L	2057.61 \pm 311.62 ^a	2.89 \pm 0.09 ^a
AS	89.81 \pm 9.66 ^b	2.73 \pm 0.07 ^a
US-1	10.21 \pm 6.79 ^c	1.84 \pm 0.3 ^b
US-2	1.47 \pm 0.57 ^d	1.19 \pm 0.31 ^c

To study the Chl-protein composition, thylakoids were isolated from the AS, US-1 and US-2 hypocotyl segments and from the leaves (as controls). Separation of the Chl-protein complexes from thylakoids by BN-PAGE (Fig. 3a) and analysis of their polypeptide composition by SDS-PAGE (Figs. 3b and c) showed the presence of the same Chl-protein bands in the leaves, the AS and the US-1 sections (Fig. 3a).

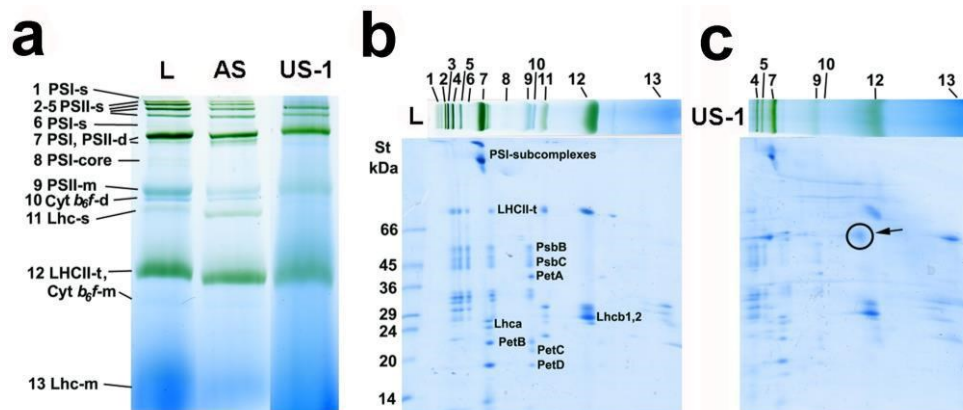


Fig. 3 Thylakoid complexes of bean leaves and hypocotyls (a): 1.D Blue-native-PAGE of thylakoids isolated from leaves (L), from the above-soil (AS) hypocotyl segments and from the uppermost under-soil (US-1) hypocotyl sections. Greenish bands are marked by numbers and identified according to their polypeptide pattern. Abbreviations: Cyt *b₆f* – cytochrome *b₆f* complex, LHC/Lhc – light-harvesting complex, PS – photosystem, s – supercomplex, t – trimer, d – dimer, m – monomer. 2.D Blue-native/SDS-PAGE of thylakoids isolated from leaves (b) and from the US-1 section (c). The polypeptides that can be easily recognized in the polypeptide patterns of the complexes are named after their genes. PSI and LHCII-t (LHCII complex) were not totally solubilized, i.e. contained Chl, even after second dimension SDS-PAGE separation. Standard (St) proteins (kDa)

were as follows: bovine serum albumin (66), ovalbumin (45), glyceraldehyde-3-phosphate dehydrogenase (36), carbonic anhydrase (29), trypsinogen (24), trypsin inhibitor (20), α -lactalbumin (14).

A spot characteristic to the US sections was cut out of the 2.D gel of the US-1 section (*c* - circled and indicated with an arrow) and was analyzed by mass spectrometry

Among the first six bands of low electrophoretic mobility, 1 and 6 were identified as supercomplexes containing PSI, though the polypeptide composition could not be resolved because of their small amounts (Fig. 3b). The polypeptide patterns of bands 2-5 indicated the presence of PSII core complexes (PsbB, PsbC) together with trimer LHCII complexes (LHCII-t) and connecting antennae of PSII, thus they were identified as PSII supercomplexes. Band 7 represented monomer PSI (PSI subcomplexes, Lhca-s) running together with dimer PSII complexes. In the faint band 8, PSI core complexes could be detected. Monomer PSII ran in band 9. Bands 11, 12 and 13 were identified as Lhc supercomplexes (LHCII-t, Lhcb-s), LHCII trimers (LHCII-t, Lhcb1, 2) and Lhc monomers, respectively. In addition to the chlorophyll-containing complexes, Cyt *b₆f* complex dimers (PetA-D) and monomer subcomplexes (PetA, PetB, PetD) were present in bands 10 and 12, respectively.

The chlorophyll-protein complex pattern was similar in leaves and in the green AS hypocotyl parts (Fig. 3a). However, some of the PSII supercomplexes (bands 2,3) and the Lhc supercomplex (band 11) could not be detected in the US-1 section (Fig. 3c). The complex pattern of the US-2 section differed a lot from the other investigated regions. We could only recognize the LHCII-t band; the other complexes did not correspond to Chl-protein complexes (see electronic supplementary material).

The positions and the polypeptide profile of the complex bands of leaves, AS and US-1 hypocotyl regions were identical, however the band densities varied. Calculating the same amount of Chl per lanes for better comparability, the amount of PSI was similar in leaves and in AS sections but showed a trend of slight decrease in the US-1 parts. The PSII gradually decreased and, in parallel, LHC increased in the AS and the US-1 regions compared to the leaves (Table 2). These results were in good agreement with the change in the Chl *a/b* ratios of the different parts (Table 1).

Table 2 Amounts of chlorophyll protein complexes in bean thylakoids isolated from the leaves (L), from the above-soil hypocotyl (AS) and from the under-soil hypocotyl sections (US-1). For comparison, the amounts are given in pixel density values (together with their SD values) normalized to identical Chl contents for better comparability. To compare the different samples, one-way ANOVAs with Tukey-Kramer *post hoc* tests were performed ($P < 0.05$)

	L	AS	US-1
PSI	24430 ± 1898 ^a	24575 ± 716 ^a	22670 ± 3241 ^a
PSII	31028 ± 1200 ^a	27848 ± 1030 ^b	24034 ± 1055 ^c
LHCII	42081 ± 2656 ^a	45198 ± 4329 ^{ab}	50021 ± 4347 ^b

The ratio of the electron transport complexes was similar in all types of thylakoids, i.e. the PSI/PSII and PSII/Cyt *b₆f* ratios showed no significant changes (Fig. 4). Neither the LHCII oligomer to monomer ratio changed significantly; however, the LHCII/PSII was elevated in the hypocotyls, particularly in the US-1 region. A marked increase in the ratio of PSII supercomplexes was observed in both the AS and US-1 section accompanied particularly by the decrease in the amount of the PSII monomers and also dimers in the latter (Fig. 4, inset).

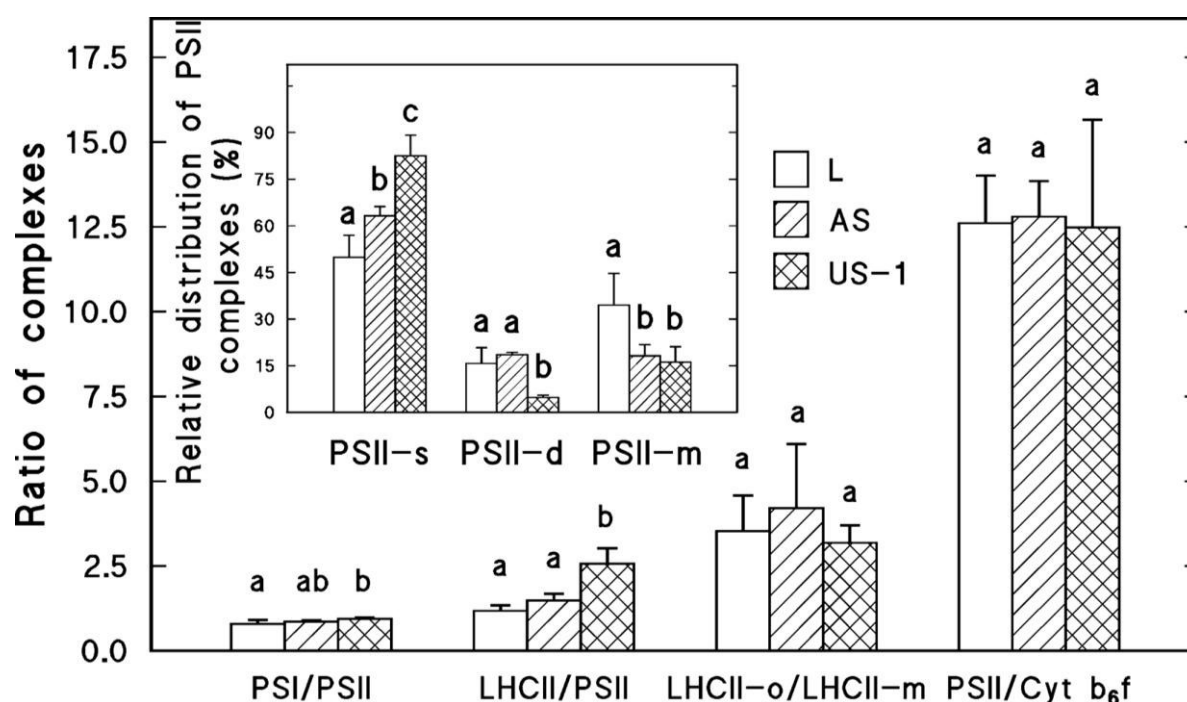


Fig. 4 Ratio of thylakoid complexes in bean leaves (L), in the above-soil hypocotyl sections (AS) and in the under-soil hypocotyl parts between 0 and 2 cm depths (US-1). Abbreviations: Cyt *b₆f* – cytochrome *b₆f* complex; LHC – light harvesting complex; PS – photosystem; o – oligomer; m – monomer. Inset: proportions (percentage distribution) of PSII complexes in thylakoids isolated from the leaf, from the AS and from the US-1 section. PSII-s - PSII supercomplexes; PSII-d - PSII dimer; PSII-m - PSII monomer. Error bars represent SD values. To compare the different samples, one-way ANOVAs with Tukey-Kramer *post hoc* tests were performed ($P < 0.05$)

The AS and US thylakoid protein patterns showed great similarity; however, the presence of a specific protein spot was observed in the 2.D BN-/SDS-PAGE protein pattern exclusively only of the US-1 sample (Fig. 3c, circled spot). To identify the nature of this protein, the spot was cut out and was analyzed with mass spectrometry which suggested that this was an aquaporin PIP-type protein (best coverage: 10.7 %).

The total protein and the thylakoid protein patterns of the different tissues and western blots for D1 protein (PsbA) and Lhc apoprotein also referred to a normal photosynthetic apparatus at least in the US-1 region (Fig. 5a). D1 protein could be only detected in the thylakoid fractions of the AS and US-1 region (Fig. 5b). ApoLhc was recognized in all hypocotyl segments, except that it was degraded in the US-2 thylakoids (Fig. 5c).

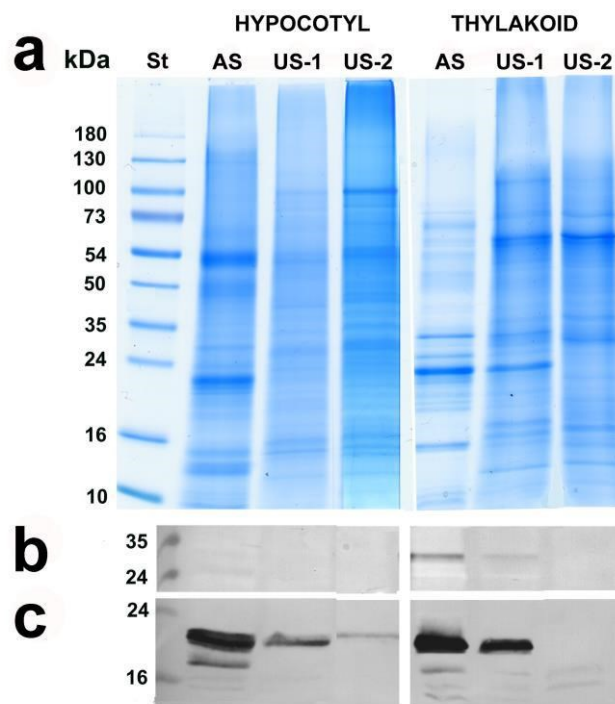


Fig. 5 Polypeptide composition of bean hypocotyl sections. *a*: polypeptide patterns (50 μg protein per lanes) of hypocotyl sections and thylakoids isolated from the above-soil hypocotyl section (AS), from the uppermost under-soil hypocotyl region (US-1) and from the lower under-soil hypocotyl region (US-2) separated by SDS-PAGE. For molecular weight estimations 10-180 kDa pre-stained Fermentas standard was used (St). *b*: Western blots against D1 (PsbA). *c*: Western blots against apoLHCII proteins

Similarities in thylakoid pigment-protein complexes of above- and under-soil parts suggested the possibility of photosynthetic activity in the latter. This was studied using variable Chl-*a* fluorescence; representative results are shown in Fig. 6. Photochemical yields of PSII (Y(II)) are presented as colour coded images (Figs. 6b and c). The regions of interest are marked in Fig. 6a which is a photo taken in infrared light as reference for orientation. The under-soil part close to the surface (US-1) had active photochemistry both in low and in high light (10 or 55 $\mu\text{mol photons m}^{-2} \text{s}^{-1}$ PFD, respectively). No photochemical activity was detected from regions deeper than 2.5 cm from the soil surface (i.e. in the US-2 and lower regions). Similarly to the AS parts, high PFD resulted in low photochemical yields in US-1 as well. In order to characterize partitioning of the energy absorbed in the chlorophyll containing

tissues, photochemical and non-photochemical yields (i.e. regulated - $Y(\text{NPQ})$ and non-regulated $Y(\text{NO})$) were measured in AS and US-1 segments of three plants, their average values are shown in Table 3.

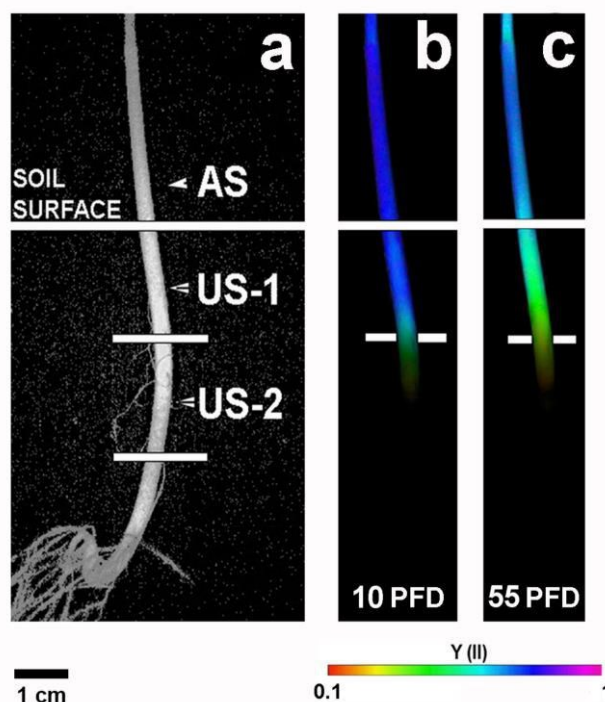


Fig. 6 Photosystem II photochemical yields $[Y(\text{II})]$ of a 14-day-old bean shoot. *a* - infrared image of the shoot with labels of the studied regions: AS - above-soil hypocotyl section, US-1 - under-soil hypocotyl segment at 0-2 cm depth, US-2 - under-soil region between 2 and 4 cm soil depths; *b* and *c* - colour coded images of $Y(\text{II})$ using 10 or 55 $\mu\text{mol photons m}^{-2} \text{s}^{-1}$ PFD blue actinic light, respectively

Low intensity ($10 \mu\text{mol photons m}^{-2} \text{s}^{-1}$ PFD) illumination did not induce $Y(\text{NPQ})$ and the absorbed energy was divided between photochemistry (PSII electron transport) and non-regulated non-photochemical quenching ($Y(\text{NO})$). The AS parts had higher photochemistry than the US-1 segments and this difference was maintained when samples were exposed to higher, $55 \mu\text{mol photons m}^{-2} \text{s}^{-1}$ PFD. In this latter experiment, $Y(\text{NPQ})$ was induced in both AS and US-1 tissues but to a higher extent in the latter (Table 3).

Table 3 Comparison of photochemical $[Y(\text{II})]$, regulated non-photochemical $[Y(\text{NPQ})]$ and non-regulated non-photochemical $[Y(\text{NO})]$ quantum yields in above-soil (AS) and under-soil hypocotyl segments at 0-2 cm depth (US-1) of a 14-day-old bean plant measured under different light intensities: $10 \mu\text{mol photons m}^{-2} \text{s}^{-1}$ PFD (10 PFD) and $55 \mu\text{mol photons m}^{-2} \text{s}^{-1}$ PFD (55 PFD). Data are means \pm standard deviations, $n=3$. Asterisks denote statistically ($P < 0.05$ in Students's t-test) significant differences between yields measured on AS and US-1 regions

	AS	US-1
10 PFD		

Y(II)	0.75 ± 0.02	$0.66 \pm 0.05^*$
Y(NPQ)	0.01 ± 0.01	0.02 ± 0.01
Y(NO)	0.24 ± 0.03	0.32 ± 0.05
<hr/>		
55 PFD		
Y(II)	0.58 ± 0.04	$0.36 \pm 0.10^*$
Y(NPQ)	0.07 ± 0.02	$0.19 \pm 0.02^*$
Y(NO)	0.35 ± 0.02	0.46 ± 0.08

In the above experiments applying low PFD, AS and US-1 regions were not significantly different concerning the Y(NO) values. Unlike light-dependent Y(NPQ) which is mainly due to ΔpH driven energy dissipation via xanthophylls [32], the biochemical realization of Y(NO) is complex consisting several different processes, some potentially leading to reactive oxygen species (ROS) production [29]. In order to investigate this non-regulated non-photochemical energy dissipation in detail, the participation of non-functional PSII reaction centers in the excitation energy (Φ_{NF}) was studied. The Φ_{NF} value of the AS region was 0.07 ± 0.01 ; however, in the US-1 sections this value increased to 0.22 ± 0.13 .

4. Discussion

The under-soil hypocotyl region is a transitional zone; it connects the above-soil photosynthesizing and the under-soil non-photosynthesizing regions. It develops as a part of the bean embryo; its length is fundamentally influenced by the sowing depth. When fully covered by soil at young seedling stage (i.e. up to the 3-4th days after germination), its tissues are fully etiolated [2]; however, when elongating and reaching the soil surface, the upper regions get green. In our previous work, we described that the hollow hypocotyl of bean pipes light into the under-soil regions. This light has a decreasing PFD gradient but allows chlorophyll formation even in 4-5 cm soil depth [7]. The question was raised if these tissues developed under dim light are photosynthetically active. This activity may influence the metabolism of the under-soil region; unlike root or hypocotyl zones fully shaded by the soil it does not depend only on the photosynthetic compounds carried from the above-soil shoot.

The presence of stomata in the epidermis of the US-1 section may allow gas exchange necessary for photosynthesis. Obviously, the regulation of the stomatal conductance might differ from that in the above-soil epidermis since these stomata are surrounded by the soil particles. The shapes of the guard cells differ from those of stomata in the above-soil region (Fig. 1) what may point to their modified activity.

No Pchl_a but low total Chl content was found in the AS hypocotyl segment (Table 1). This proves that the light piped into the US-1 region causes regular Pchl_a

phototransformation. This low Chl content must be the consequence of the low PFD value and the spectral composition of the piped light. The spectral characteristics of the piped light differ from those of the direct sunlight; the ratio of the near infrared region is high [7] which resembles inner-canopy light quality. Far-red or near infrared light is conducted by plant tissues [33,18] and is effectively transmitted by most soil types [34]. As a result, this light can regulate the hypocotyl development in the soil [35].

Interestingly, despite of the great differences in the amounts of Chls and thus the Chl-protein complex contents of leaves, AS and US-1 hypocotyl segments, only minor differences were found in the Chl-protein complex ratios and only minor differences were shown in the Chl *a/b* ratios of leaves and AS sections (Table 1). The relative amounts of PSII were higher in supercomplexes (oligomers) in the US-1 region than in AS (Fig. 4). This kind of arrangement is important for efficient energy transfer under low-light conditions [36]. The far-red wavelengths are mainly absorbed by PSI thus the relative increase in the LHCII to PSII ratio along with the lower Chl-*a* to Chl-*b* ratio in low-light adapted plants is suggested to ensure an efficient electron supply of PSI [11,8]. These are general characteristics of plants grown under low-light conditions [11,37,17]. The Chl-protein composition observed in the US-1 region showed similarity to that of greening roots [38], but the organization of the antennae was normal in the bean hypocotyl according to the fluorescence emission spectra of the different hypocotyl regions [7]. The reorganization of thylakoid complexes, i.e. the higher PSII supercomplex ratio in US-1 may also have a role in the excess light energy dissipation in case of occasional high PFD illumination [39]. However, this defense system is not effective in etiolated stem related organs. Etiolated pea epicotyls exposed to direct sunshine undergo photodegradation processes [40,41] caused by ROS production [42,43].

An interesting feature of the under-soil hypocotyl section was the 66 kD protein detected in the thylakoids (Fig. 3c) that was identified as a PIP-type aquaporin. Aquaporins were isolated earlier from the thylakoid fraction of *Nicotiana* leaf chloroplasts [44] but their beneficial function is still questioned [45]. Aquaporin family proteins facilitate not only water transport but they are also transporters of CO₂ [47,48,49] and H₂O₂ [49]. In the light sensitive hypocotyl sections, the transport of H₂O₂ may have important role not only in protecting the thylakoid membranes by regulating the redox state in its environment but also in the signalization of the oxidative stress processes [50].

The Chl-*a* fluorescence induction measurements demonstrated that the observed structural similarities between US-1 and photosynthetic AS tissues were reflected in PSII photochemistry (Fig. 6). Hypocotyls adapted to very low light in the upper region of soil

showed smaller but significant PSII electron transport when taken from the soil and illuminated in the laboratory. Relative differences between PSII photochemistry of US-1 and AS segments were more pronounced when probed by higher actinic light (Fig. 6c, Table 3). However, US-1 segments could also cope with this light irradiation. In contrast, Mahmudov et al. [51] showed that under the greening process of etiolated wheat leaves, higher than saturating PFD induced a significant PSII inactivation as a result of incomplete incorporation of quinone acceptors in the PSII reaction centers. Since there was a significant enhancement in the Y(NPQ) in US-1 segments under high PFD compared to low PFD illumination, the photosynthetic apparatus present in the US-1 segment was capable for light acclimation and xanthophyll-cycle based quenching processes, typical to well-operating photosynthetic machineries. Increase in the Y(NPQ) was also found during late stages of the greening process in wheat leaves [52]. Reaction center quenching is a process of primary importance if the acceptor-side processes in the PSII are limited by different reasons [53]. Here, more than 20% of the PSII reaction centers became inactivated and the energy was emitted as heat and fluorescence. This excess energy may lead to the generation of ROS which, (unless neutralized by antioxidants in protective pathways - such as the water-water cycle (Mehler-Asada pathway [54])), may be transported as H₂O₂ through the aquaporins identified in the under-soil tissues (Fig. 3c).

Chloroplasts were present in the xylem, phloem and pith parenchyma cells (Fig. 2) but they differed from the typical plastids of leaves. The presence of starch grains and low grana are characteristics of high-light adapted plastids [55,12] while the absence or rare appearance of starch grains, high stacking degree of thylakoids and high grana (16 in average) were found in leaves developed under low-light conditions [56]. The plastids in the US-1 showed diverse features: large starch grains were usually found and the stacking degree was less than 10 thylakoids per grana; these grana were broad. This mixed feature of the chloroplasts can be due to a “double feeding” of the cells in the US-1 segment; besides their own photosynthetic activity, sugars are transported from the above-soil shoot sources towards the lower hypocotyls segments and the root as sinks.

The results of this paper prove that the general concept about the source role of the above-soil shoot and sink function of the under-soil tissues should be modified. The cells in the under-soil region must be supplied *via* phloem transport with photosynthesis products of the shoot but the light piped by the above-soil organs (by the hollow hypocotyl in the case of bean) activates the formation of a low-light adapted active photosynthetic apparatus, too.

Author contribution statement

B.B. conceptualized the study, designed and coordinated the experiments. A.K. participated in all experimental work and compiled the manuscript with contributions from all authors. É.S. performed the proteomic studies and analyzed the data. É.H.G. carried out the mass spectrometry. Á.S., Gy.Cz. and É.H. performed the Chl-*a* fluorescence induction kinetics and imaging measurements. K.B. performed the electron microscopic studies. All authors have read, discussed and approved the submitted manuscript.

Acknowledgements

The authors are grateful to Csilla Jónás and Zsuzsanna Ostorics for their technical assistance. Á. Solti was also supported by the Bolyai János Research Scholarship of the Hungarian Academy of Sciences (BO/00207/15/4).

References

- [1] Woolley, J. T. & Stoller, E. W. (1978). Light penetration and light-induced seed germination in soil. *Plant Physiology*, 61(4): 597-600.
- [2] Vitányi, B., Kósa, A., Solymosi, K. & Böddi, B. (2013). Etioplasts with protochlorophyll and protochlorophyllide forms in the under-soil epicotyl segments of pea (*Pisum sativum*) seedlings grown under natural light conditions. *Physiologia Plantarum*, 148(2): 307-315.
- [3] Griffiths, W. T. (1978). Reconstitution of chlorophyllide formation by isolated etioplast membranes. *Biochemical Journal*, 174: 681-692.
- [4] Shibata, K. (1957). Spectroscopic studies on chlorophyll formation in intact leaves. *The Journal of Biochemistry*, 44(3): 147-173.
- [5] Böddi, B., Ryberg, M. & Sundqvist, C. (1992). Identification of four universal protochlorophyllide forms in dark-grown leaves by analyses of the 77 K fluorescence emission spectra. *Journal of Photochemistry and Photobiology B: Biology*, 12(4): 389-401.
- [6] Böddi, B., McEwen, B., Ryberg, M. & Sundqvist, C. (1994). Protochlorophyllide forms in non-greening epicotyls of dark-grown pea (*Pisum sativum*). *Physiologia Plantarum*, 92(1): 160-170.
- [7] Kakuszi, A. & Böddi, B. (2014). Light piping activates chlorophyll biosynthesis in the under-soil hypocotyl section of bean seedlings. *Journal of Photochemistry and Photobiology B: Biology*, 140: 1-7.
- [8] Walters, R. G. (2005). Towards an understanding of photosynthetic acclimation. *Journal of Experimental Botany*, 56(411): 435-447.

- [9] Rochaix, J. D. (2014). Regulation and dynamics of the light-harvesting system. *Annual Review of Plant Biology*, 65: 287-309.
- [10] Leong, T. Y. & Anderson, J. M. (1984). Adaptation of the thylakoid membranes of pea chloroplasts to light intensities. I. Study on the distribution of chlorophyll-protein complexes. *Photosynthesis Research*, 5(2): 105-115.
- [11] Walters, R. G. & Horton, P. (1994). Acclimation of *Arabidopsis thaliana* to the light environment: changes in composition of the photosynthetic apparatus. *Planta*, 195(2): 248-256.
- [12] Lichtenthaler, H. K., Kuhn, G., Prenzel, U., Buschmann, C. & Meier, D. (1982). Adaptation of chloroplast-ultrastructure and of chlorophyll-protein levels to high-light and low-light growth conditions. *Zeitschrift für Naturforschung C*, 37(5-6): 464-475.
- [13] Anderson, J. M., Chow, W. S. & Goodchild, D. J. (1988). Thylakoid membrane organization in sun/shade acclimation. *Functional Plant Biology*, 15(2): 11-26.
- [14] Nilsen, E. T. & Sharifi, M. R. (1994). Seasonal acclimation of stem photosynthesis in woody legume species from the Mojave and Sonoran deserts of California. *Plant Physiology*, 105(4): 1385-1391.
- [15] Saveyn, A., Steppe, K., Ubierna, N. & Dawson, T. E. (2010). Woody tissue photosynthesis and its contribution to trunk growth and bud development in young plants. *Plant, Cell & Environment*, 33(11): 1949-1958.
- [16] Dima, E., Manetas, Y. & Psaras, G. K. (2006). Chlorophyll distribution pattern in inner stem tissues: evidence from epifluorescence microscopy and reflectance measurements in 20 woody species. *Trees*, 20(4): 515-521.
- [17] Wittmann, C. & Pfanz, H. (2015). The optical, absorptive and chlorophyll fluorescence properties of young stems of five woody species. *Environmental and Experimental Botany*, 121: 83-93.
- [18] Mandoli, D. F. & Briggs, W. R. (1984). Fiber-optic plant tissues: spectral dependence in dark-grown and green tissues. *Photochemistry and Photobiology*, 39(3): 419-424.
- [19] Reynolds, E. S. (1963). The use of lead citrate at high pH as an electron-opaque stain in electron microscopy. *The Journal of Cell Biology*, 17(1): 208-212.
- [20] Porra, R.J., Thompson, W.A. & Kriedemann, P.E. (1989). Determination of accurate extinction coefficients and simultaneous equations for assaying chlorophyll *a* and *b* extracted with four different solvents: verification of the concentration of chlorophyll standards by atomic absorption spectroscopy. *Biochimica et Biophysica Acta (BBA)*, 975: 384-394.

- [21] Sárvári, É., Mihailova, G., Solti, Á., Keresztes, Á., Velitchkova, M. & Georgieva, K. (2014). Comparison of thylakoid structure and organization in sun and shade *Haberlea rhodopensis* populations under desiccation and rehydration. *Journal of Plant Physiology*, *171*: 1591–1600.
- [22] Laemmli, U.K. (1970). Cleavage of structural proteins during assembly of the head of bacteriophage T4. *Nature*, *227*: 680–685.
- [23] Candiano, G., Bruschi, M., Musante, L., Santucci, L., Ghiggeri, G.M., Carnemolla, B., Orecchia, P., Zardi, L. & Righetti, P.G. (2004). Blue silver: a very sensitive colloidal Coomassie G-250 staining for proteome analysis. *Electrophoresis*, *25*: 1327–1333.
- [24] Suh, H.J., Kim, C.S. & Jung, J. (2000). Cytochrome *b₆/f* complex as an indigenous photodynamic generator of singlet oxygen in thylakoid membranes. *Photochemistry and Photobiology*, *71*: 103–109.
- [25] Aro, E.M., Suorsa, M., Rokka, A., Allahverdiyeva, Y., Paakkarinen, V., Saleem, A., Battchikova, N. & Rintamäki, E. (2005). Dynamics of photosystem II: a proteomic approach to thylakoid protein complexes. *Journal of Experimental Botany*, *56*: 347–356.
- [26] Nelson, N. & Yocum, C.F. (2006). Structure and function of photosystem I and II. *Annual Review of Plant Biology*, *57*: 521–565.
- [27] Basa, B., Lattanzio, G., Solti, Á., Tóth, B., Abadía, J., Fodor, F. & Sárvári, É. (2014). Changes induced by cadmium stress and iron deficiency in the composition and organization of thylakoid complexes in sugar beet (*Beta vulgaris* L.). *Environmental and Experimental Botany*, *101*: 1–11.
- [28] Szenzenstein, A., Kósa, A., Solymosi, K., Sárvári, É. & Böddi, B. (2010). Preferential regeneration of the NADPH: protochlorophyllide oxidoreductase oligomer complexes in pea epicotyls after bleaching. *Physiologia Plantarum*, *138*: 102–112.
- [29] Klughammer, C. & Schreiber, U. (2008). Complementary PS II quantum yields calculated from simple fluorescence parameters measured by PAM fluorometry and the Saturation Pulse method. *PAM Application Notes*, *1*(2): 27–35.
- [30] Hendrickson, L., Förster, B., Pogson, B.J. & Chow, W.S. (2005). A simple chlorophyll fluorescence parameter that correlates with the rate coefficient of photoinactivation of Photosystem II. *Photosynthesis Research*, *84*: 43–49.
- [31] Solti, Á., Lenk, S., Mihailova, G., Mayer, P., Barócsi, A. & Georgieva, K. (2014). Effects of habitat light conditions on the excitation quenching pathways in desiccating *Haberlea rhodopensis* leaves: an Intelligent FluoroSensor study. *Journal of Photochemistry and Photobiology B: Biology*, *130*: 217–225.

- [32] Demmig, B., Winter, K., Krüger, A. & Czygan, F. C. (1987). Photoinhibition and zeaxanthin formation in intact leaves a possible role of the xanthophyll cycle in the dissipation of excess light energy. *Plant Physiology*, 84(2): 218-224.
- [33] Kasperbauer, M. J. (1971). Spectral distribution of light in a tobacco canopy and effects of end-of-day light quality on growth and development. *Plant Physiology*, 47(6): 775-778.
- [34] Bliss, D. & Smith, H. (1985). Penetration of light into soil and its role in the control of seed germination. *Plant, Cell & Environment*, 8(7): 475-483.
- [35] Von Arnim, A. & Deng, X.W. (1996). Light control of seedling development. *Annual Review of Plant Biology*, 47(1): 215-243.
- [36] Kouřil, R., Wientjes, E., Bultema, J. B., Croce, R., & Boekema, E. J. (2013). High-light vs. low-light: effect of light acclimation on photosystem II composition and organization in *Arabidopsis thaliana*. *Biochimica et Biophysica Acta (BBA)-Bioenergetics*, 1827(3): 411-419.
- [37] Solymosi, K., Bóka, K. & Böddi, B. (2006). Transient etiolation: protochlorophyll (ide) and chlorophyll forms in differentiating plastids of closed and breaking leaf buds of horse chestnut (*Aesculus hippocastanum*). *Tree Physiology*, 26(8): 1087-1096.
- [38] Kobayashi, K., Sasaki, D., Noguchi, K., Fujinuma, D., Komatsu, H., Kobayashi, M., Sato, M., Toyooka, K., Sugimoto, K., Niyogi, K.K. & Wada, H. (2013). Photosynthesis of root chloroplasts developed in *Arabidopsis* lines overexpressing GOLDEN2-LIKE transcription factors. *Plant and cell physiology*, 54(8): 1365-1377.
- [39] Bailey, S., Walters, R. G., Jansson, S. & Horton, P. (2001). Acclimation of *Arabidopsis thaliana* to the light environment: the existence of separate low light and high light responses. *Planta*, 213(5): 794-801.
- [40] Erdei, N., Barta, C., Hideg, É. & Böddi, B. (2005). Light-induced wilting and its molecular mechanism in epicotyls of dark-germinated pea (*Pisum sativum* L.) seedlings. *Plant and Cell Physiology*, 46(1): 185-191.
- [41] Hideg, É., Vitányi, B., Kósa, A., Solymosi, K., Bóka, K., Won, S., Inoue, Y., Ridge, R.W. & Böddi, B. (2010). Reactive oxygen species from type-I photosensitized reactions contribute to the light-induced wilting of dark-grown pea (*Pisum sativum*) epicotyls. *Physiologia Plantarum*, 138(4): 485-492.
- [42] Standfuss, J., van Scheltinga, A. C. T., Lamborghini, M. & Kühlbrandt, W. (2005). Mechanisms of photoprotection and nonphotochemical quenching in pea light-harvesting complex at 2.5 Å resolution. *The EMBO Journal*, 24(5): 919-928.
- [43] Li, Z., Wakao, S., Fischer, B. B. & Niyogi, K. K. (2009). Sensing and responding to excess light. *Annual Review of Plant Biology*, 60: 239-260.

- [44] Ferro, M., Brugière, S., Salvi, D., Seigneurin-Berny, D., Moyet, L., Ramus, C., Miras, S., Mellal, M., Le Gall, S., Kieffer-Jaquinod, S. & Bruley, C. (2010). AT_CHLORO, a comprehensive chloroplast proteome database with subplastidial localization and curated information on envelope proteins. *Molecular & Cellular Proteomics*, 9(6): 1063-1084.
- [45] Beebo, A., Mathai, J. C., Schoefs, B. & Spetea, C. (2013). Assessment of the requirement for aquaporins in the thylakoid membrane of plant chloroplasts to sustain photosynthetic water oxidation. *FEBS Letters*, 587(14): 2083-2089.
- [46] Terashima, I. & Ono, K. (2002). Effects of HgCl₂ on CO₂ dependence of leaf photosynthesis: evidence indicating involvement of aquaporins in CO₂ diffusion across the plasma membrane. *Plant and Cell Physiology*, 43(1): 70-78.
- [47] Uehlein, N., Lovisolò, C., Siefritz, F. & Kaldenhoff, R. (2003). The tobacco aquaporin NtAQP1 is a membrane CO₂ pore with physiological functions. *Nature*, 425(6959): 734-737.
- [48] Uehlein, N., Otto, B., Hanson, D. T., Fischer, M., McDowell, N. & Kaldenhoff, R. (2008). Function of *Nicotiana tabacum* aquaporins as chloroplast gas pores challenges the concept of membrane CO₂ permeability. *The Plant Cell*, 20(3): 648-657.
- [49] Bienert, G. P. & Chaumont, F. (2014). Aquaporin-facilitated transmembrane diffusion of hydrogen peroxide. *Biochimica et Biophysica Acta (BBA)-General Subjects*, 1840(5): 1596-1604.
- [50] Maruta, T., Noshi, M., Tanouchi, A., Tamoi, M., Yabuta, Y., Yoshimura, K., Ishikawa, T. & Shigeoka, S. (2012). H₂O₂-triggered retrograde signaling from chloroplasts to nucleus plays specific role in response to stress. *Journal of Biological Chemistry*, 287(15): 11717-11729.
- [51] Mahmudov, Z. M., Abdullayev, K. D. & Gasanov, R. A. (2005). Photoinhibition in vivo of Photosystem II reactions during development of the photosystems of wheat seedlings. *Photosynthesis Research*, 84(1-3): 9-14.
- [52] Garmash, E. V., Dymova, O. V., Malyshev, R. V., Plyusnina, S. N. & Golovko, T. K. (2013). Developmental changes in energy dissipation in etiolated wheat seedlings during the greening process. *Photosynthetica*, 51(4): 497-508.
- [53] Huner, N. P., Ivanov, A. G., Sane, P. V., Pockock, T., Krol, M., Balseris, A., Rosso, D., Savitch, L.V., Hurry, V.M. & Öquist, G. (2008). Photoprotection of photosystem II: reaction center quenching versus antenna quenching. In *Photoprotection, Photoinhibition, Gene Regulation, and Environment, Advances in Photosynthesis and Respiration Vol. 21*, Springer, The Netherlands, pp 155-173.

[54] Asada, K. (1999). The water-water cycle in chloroplasts: scavenging of active oxygens and dissipation of excess photons. *Annual Review of Plant Biology*, 50(1): 601-639.

[55] Lichtenthaler, H. K., Buschmann, C., Döll, M., Fietz, H. J., Bach, T., Kozel, U., Meier, D. & Rahmsdorf, U. (1981). Photosynthetic activity, chloroplast ultrastructure and leaf characteristics of high-light and low-light plants and of sun and shade leaves. *Photosynthesis Research*, 2(2): 115-141.

[56] Lichtenthaler, H. K., Meier, D. & Buschman C. (1984). Development of chloroplasts at high and low light quanta fluence rates. *Israel Journal of Botany*, 33: 185-194.